

Received 18 July 2024

Accepted 18 September 2024

Edited by A. Briceno, Venezuelan Institute of
Scientific Research, Venezuela**Keywords:** crystal structure; Hirshfeld surface analysis; C—H···Cl hydrogen bond; phenanthroline; tin(IV).**CCDC reference:** 2370790**Supporting information:** this article has supporting information at journals.iucr.org/e

Crystal structure and Hirshfeld surface analysis of trichlorido(1,10-phenanthroline- $\kappa^2 N,N'$)phenyl-tin(IV)

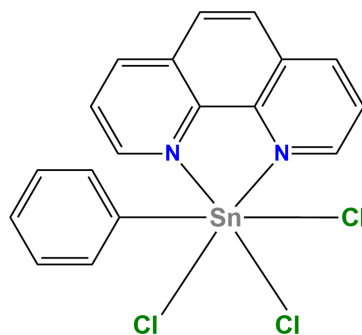
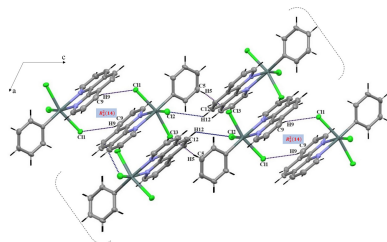
Tarek Benlatreche,^{a,b*} Mohamed Abdellatif Bensegueni,^a Georges Dénès,^c Stéphane Golhen^d and Hocine Merazig^a

^aEnvironmental and Structural Molecular Chemistry Research Unit, URCHEMS, Faculty of Exact Sciences, University of Constantine 1-Mentouri Brothers, 25000, Algeria, ^bNational Higher School for Hydraulics, Abdellah Arbaoui, Blida, Algeria, ^cLaboratory of Solid State Chemistry and Mössbauer Spectroscopy, Chemistry and Biochemistry Department, Concordia University, Montreal, Canada, and ^dCNRS, Rennes Institute of Chemical Sciences – UMR 6226, University of Rennes, France. *Correspondence e-mail: t.benlatreche@ensh.dz

The title compound, $[Sn(C_6H_5)Cl_3(C_{12}H_8N_2)]$, which was obtained by the reaction between 1,10-phenanthroline and phenyltin trichloride in methanol, exhibits intramolecular hydrogen-bonding interactions involving the chlorine and hydrogen atoms. Crystal cohesion is ensured by intermolecular C—H···Cl hydrogen bonds, as well as $Y—X\cdots\pi$ and π -stacking interactions involving three different aromatic rings with centroid–centroid distances of 3.6605 (13), 3.9327 (14) and 3.6938 (12) Å]. Hirshfeld surface analysis and the associated two-dimensional fingerprint plots reveal significant contributions from H···H (30.7%), Cl···H/H···Cl (32.4%), and C···H/H···C (24.0%) contacts to the crystal packing while the C···C (6.2%), C···Cl/Cl···C (4.1%), and N···H/H···N (1.7%) interactions make smaller contributions.

1. Chemical context

Complexes of 1,10-phenanthroline (Phen) with *d*-metals have attracted much interest because of the adaptability and chemical properties of Phen (Sammes & Yahioglu, 1994), that confers additional properties upon coordination with other metals and thus opens up new areas of investigation. Tin(IV) complexes are widespread in chemistry and play a significant role in biology, industry, and agriculture (Syed Annuar *et al.*, 2021; Ross, 2006) as this class of compounds has shown efficacy against a wide range of diseases and they have strong biological activities such as antifungal (Rebolledo *et al.*, 2003), antibacterial (Al-Allaf *et al.*, 2003), anti-proliferative and antitumor (Banti *et al.*, 2019) properties.



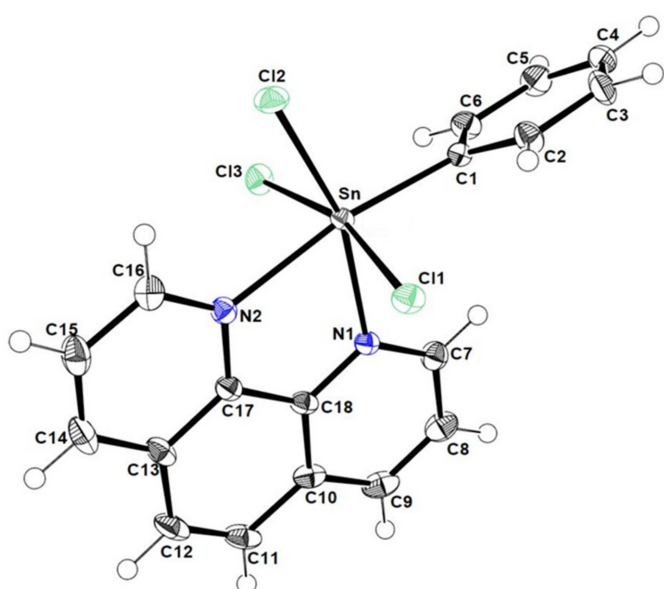
The synthesis of the title compound along with the crystal structure and spectroscopic characterization, as well as the results of a Hirshfeld surface analysis are all reported here.

Table 1Selected geometric parameters (\AA , $^\circ$).

Sn1—Cl3	2.4530 (6)	Sn1—N2	2.2728 (19)
Sn1—Cl1	2.4419 (6)	Sn1—N1	2.2802 (19)
Sn1—Cl2	2.4067 (6)	Sn1—C1	2.145 (2)
Cl1—Sn1—Cl3	165.07 (2)	N2—Sn1—N1	72.77 (7)
Cl2—Sn1—Cl3	91.82 (2)	N1—Sn1—Cl3	85.10 (5)
Cl2—Sn1—Cl1	93.08 (2)	N1—Sn1—Cl1	86.12 (5)
N2—Sn1—Cl3	82.62 (5)	N1—Sn1—Cl2	163.04 (5)
N2—Sn1—Cl1	83.27 (5)	C1—Sn1—N2	168.92 (8)
N2—Sn1—Cl2	90.30 (5)		

2. Structural commentary

The title complex (Fig. 1) crystallizes in the monoclinic space group $P2_1/n$. Bond lengths and angles are comparable with those previously reported for related structures (Hall *et al.*, 1996). The tin atom is six-coordinate, being chelated by two nitrogen atoms (N1 and N2) of the 1,10-phenanthroline ligand and coordinated by a carbon atom of the phenyl ligand (C1), and three chlorine atoms (Table 1). The geometry of the tin atom is distorted octahedral with angles ranging from 72.77 (7) to 168.92 (8) $^\circ$, the smallest being between the tin atom and the two nitrogen atoms and the largest is between the tin and carbon atom of the phenyl and the nitrogen atom of the ligand. The dihedral angle between the planes through the phenyl ring and the phenanthroline ligand is 69.73 (9) $^\circ$. Intramolecular C—H \cdots Cl hydrogen bonds are observed (Table 2), characterized by $D\cdots A$ distances of 2.75, 2.86 and 2.97 \AA . These interactions play a vital role in maintaining the specific conformation of the molecule, thus enhancing its overall rigidity (Fig. 2).

**Figure 1**

The asymmetric unit of the title compound with displacement ellipsoids drawn at the 50% probability level. H atoms are represented as small circles.

Table 2Hydrogen-bond geometry (\AA , $^\circ$).

$D\cdots H\cdots A$	$D\cdots H$	$H\cdots A$	$D\cdots A$	$D\cdots H\cdots A$
C15—H15 \cdots Cl3 ⁱ	0.95	2.94	3.851 (1)	139
C5—H5 \cdots Cl3 ⁱⁱ	0.95	2.84	3.773 (2)	166
C9—H9 \cdots Cl1 ⁱⁱⁱ	0.95	2.87	3.683 (2)	144
C2—H2 \cdots Cl1	0.95	2.75	3.392 (2)	126
C6—H6 \cdots Cl3	0.95	2.86	3.411 (1)	124
C16—H16 \cdots Cl2	0.95	2.97	3.328 (3)	126
C7—H7 \cdots Cl2 ^{iv}	0.95	2.85	3.654 (1)	143
C12—H12 \cdots Cl2 ^v	0.95	2.97	3.693 (4)	133

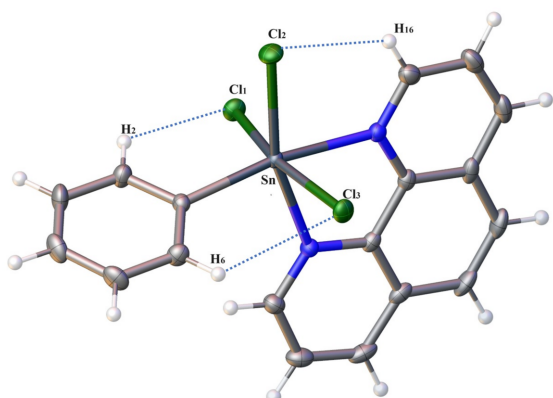
Symmetry codes: (i) $-x + \frac{3}{2}, y + \frac{1}{2}, -z + \frac{3}{2}$; (ii) $-x + 1, -y + 1, -z + 2$; (iii) $-x + 1, -y + 1, -z + 1$; (iv) $-x + \frac{1}{2}, y - \frac{1}{2}, -z + \frac{3}{2}$; (v) $x + \frac{1}{2}, -y + \frac{3}{2}, z - \frac{1}{2}$.

3. Supramolecular features

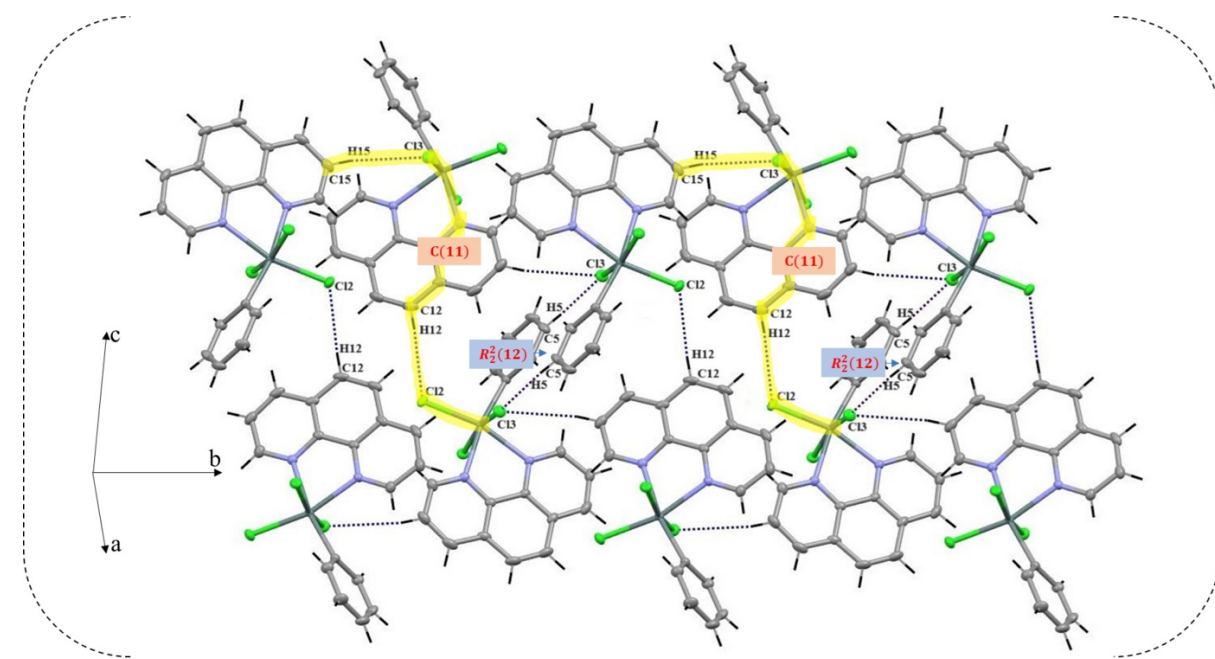
The crystal structure is intricately organized, primarily upheld by weak intermolecular C—H \cdots Cl hydrogen bonds (Table 3), $Y\cdots X\cdots\pi$ and π -stacking interactions. These interactions act as the framework for structural cohesion, effectively connecting individual molecules.

Within this framework, the intermolecular C15—H15 \cdots Cl3, C5—H5 \cdots Cl3 and C12—H12 \cdots Cl2 hydrogen bonds, with the H \cdots A distances of 2.94, 2.84 and 2.97 \AA , respectively, create bridges between adjacent molecules. These hydrogen bonds generate rings with an $R_2^2(12)$ motif and $C(11)$ chains (Etter *et al.*, 1990), which align along the b -axis direction, creating hydrogen-bonded planes parallel to the ab plane (Fig. 3) (Etter *et al.*, 1990). These planes, in turn, are linked along the c -axis by C9—H9 \cdots Cl1 hydrogen bonds generating $R_2^2(14)$ hydrogen-bonded rings (Fig. 4); this bonding mechanism facilitates cohesion and contributes to the consolidation of the crystal structure.

The three-dimensional architecture is further consolidated by π -stacking interactions between 1,10-phenanthroline units, with centroid–centroid distances $Cg2\cdots Cg2(1-x, 1-y, 1-z) = 3.9327 (14)$ \AA and $Cg1\cdots Cg2(1-x, 1-y, 1-z) = 3.6605 (13)$ \AA where $Cg2$ and $Cg1$ are the centroids of the N1/C7-C10/C18 and C10-C13/C17/C18 rings, respectively.

**Figure 2**

Intramolecular hydrogen bonds directing the conformation of the structure.

**Figure 3**

Intermolecular hydrogen bonds: C15—H15···Cl3ⁱ, C5—H5···Cl3ⁱⁱ, and C12—H12···Cl2^v and hydrogen-bonded planes in the title compound. [Symmetry codes: (i) $-x + \frac{3}{2}, y + \frac{1}{2}, -z + \frac{3}{2}$; (ii) $-x + 1, -y + 1, -z + 2$; (v) $x + \frac{1}{2}, -y + \frac{3}{2}, z - \frac{1}{2}$]

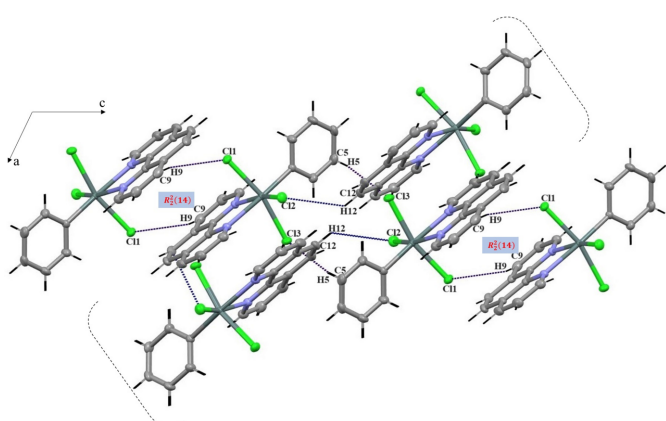
Additionally, $Y-X\cdots\pi$ interactions, Sn1—Cl2···Cg3($\frac{1}{2} - x, \frac{1}{2} + y, \frac{3}{2} - z$), where Cg3 is the centroid of the C1—C6 ring, with a Cl···Cg distance of 3.6938 (12) Å, create extra connections within the crystal (Fig. 5).

Remarkably, despite the intricate network of interactions, no classical hydrogen bonds or voids are detected within the structure, underscoring the efficiency of the aforementioned mechanisms in maintaining structural cohesion.

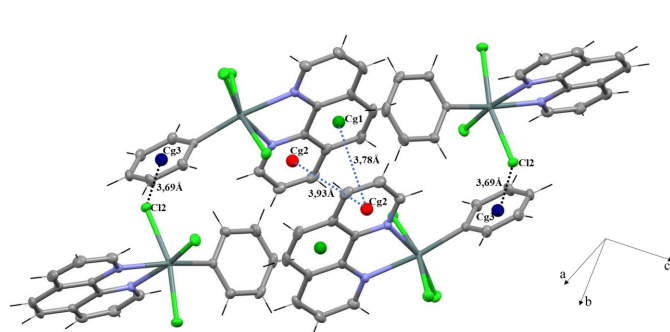
4. Database survey

A search of the Cambridge structural Database (CSD, version 2024.2.0, update of September 2024; Groom *et al.*, 2016) for

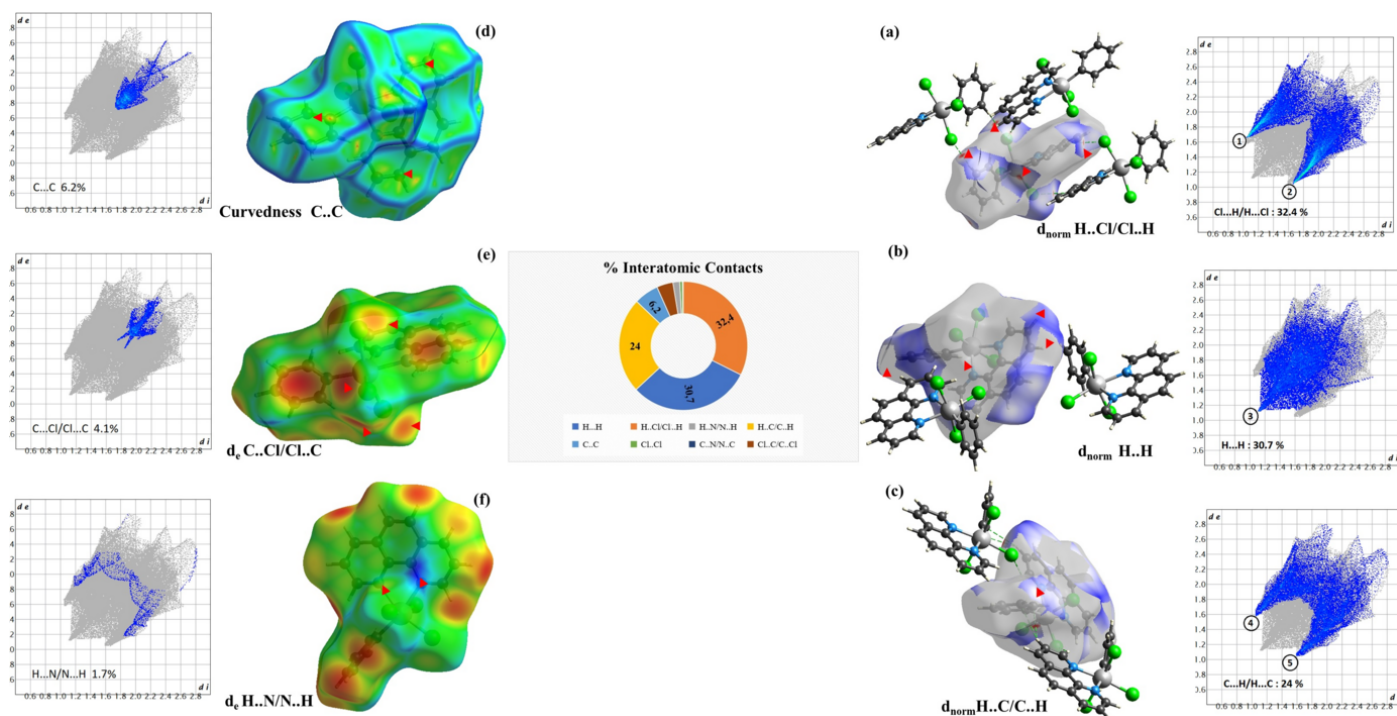
similar compounds was undertaken. The compound CEXMIC (Su *et al.*, 2007) crystallizes with the same arrangement, differing only in the substitution of the phenyl ligand with a chloro substituent. This is also observed in TECMUJ (Hall & Tiekkink, 1996), but with a different arrangement in the $P\bar{1}$ space group of the triclinic crystal system. Similarly, in ARAWOF (Casas *et al.*, 2003), with space group $P2_1/n$, an ethyl group replaces the Cl atom in the coordination sphere while maintaining the same crystalline structure. CIHQUI (Klössener *et al.*, 2018) crystallizes with an identical crystal structure but exhibits halogen interactions and hydrogen bonding with a fluorine atom as the generator atom. AYAFEL (Ma *et al.*, 2004) crystallizes with space group $Pca2_1$, featuring two chelations, one with the same ligand and another with a sulfur ligand, while the chloro substituents are substituted with methyls. Compound BOVHUQ (Tan *et al.*, 2009) crystallizes in the same space group, with both chloro and phenyl ligands

**Figure 4**

Linkage of planes along the c axis by C9—H9···Cl1ⁱⁱⁱ hydrogen bonds, forming R₂²(14) rings. [Symmetry code: (iii) $-x + 1, -y + 1, -z + 1$.]

**Figure 5**

π -stacking and $Y-X\cdots\pi$ interactions between 1,10-phenanthroline rings, reinforcing the structure.

**Figure 6**

Hirshfeld surface analysis and two-dimensional fingerprints. (a) Hirshfeld surface showing $\text{Cl}\cdots\text{H}/\text{H}\cdots\text{Cl}$ interactions with red spots indicating close $\text{H}\cdots\text{Cl}$ contacts; white areas match van der Waals radii distances. (b) Hirshfeld surface showing $\text{H}\cdots\text{H}$ contacts. (c) two-dimensional fingerprint of $\text{C}\cdots\text{H}/\text{H}\cdots\text{C}$ contacts in d_{norm} mode. (d) Curvedness HS indicating contacts between carbon atoms, showing the π -stacking interactions. (e) Shape-index plot indicating $\text{C}\cdots\text{Cl}/\text{Cl}\cdots\text{C}$ interactions; (f) shape-index plot indicating $\text{H}\cdots\text{N}/\text{N}\cdots\text{H}$ interactions.

substituted with halogenated ligands. CASVOH (Ganis *et al.*, 1983), in orthorhombic space group $P2_12_12_1$, features chloro and phenyl ligands substituted with *n*-butyl. Similarly, in DUKTAH (Lo *et al.*, 2020), the substitution ligand is 4-chlorophenyl. In EDUNYEY (Najafi *et al.*, 2012) the chloro ligands are replaced by methyl and SCN ligands. FEDYIW (Archer *et al.*, 1987) exhibits a coordination of 4. RORMIU (Lange *et al.*, 1997) is a polymeric compound while SIZBIO (Najafi *et al.*, 2014), NEMTAB (Davis *et al.*, 2006), POYZAE (Kircher *et al.*, 1998) and TECMUJ (Hall *et al.*, 1996) include organic co-crystals in their crystal structures. Similar structures are observed for PAPTOPS, PAPTRY, PAPVAG, and PAPVEK (Mo *et al.*, 2017), but with different halogen-halogen interactions.

5. Hirshfeld surface analysis

To investigate the nature of intermolecular interactions and their importance in the crystal packing, a Hirshfeld surface (HS) analysis was undertaken and associated two-dimensional fingerprint plots (FP) (Spackman & Jayatilaka, 2009) were generated using *Crystal Explorer 21.5* (Turner *et al.*, 2021). The Hirshfeld surfaces were generated with high (standard) surface resolution and the 3-D d_{norm} surfaces were mapped using a fixed color scale ranging from 0.76 (red) to 2.4 (blue) from -0.0947 to 1.3214 Å. The 2D fingerprint plots were displayed using the expanded $1.0\text{--}2.8$ Å view with distance scales d_e and d_i depicted on the graph axes.

In Fig. 6a, the red spots indicate close $\text{H}\cdots\text{Cl}$ contacts, which can be attributed to the $\text{C}-\text{H}\cdots\text{Cl}$ hydrogen bonds. The white and red areas represent regions where the distance between neighboring atoms closely matches the sum of their van der Waals radii, suggesting $\text{H}\cdots\text{Cl}$ contacts. Blue areas indicate instances where neighboring atoms are too distant to interact. The 2D FP plot displayed in Fig. 6a illustrates the $\text{H}\cdots\text{Cl}/\text{Cl}\cdots\text{H}$ contacts, which make the most significant contribution to the total Hirshfeld surface area (32.4%). It is characterized by two symmetrical peaks at the top left and bottom right with $d_e + d_i = 2.7$ Å (labeled 1 and 2).

Fig. 6b and 6c illustrate the $\text{H}\cdots\text{H}$ contacts and $\text{C}\cdots\text{H}/\text{H}\cdots\text{C}$ contacts respectively, represented by red dots. The 2D FP shown in Fig. 6b shows the two-dimensional (d_i , d_e) points associated with hydrogen atoms ($\text{rvdW} = 1.20$ Å). It features an endpoint towards the origin with $d_i = d_e = 1.1$ Å (labeled 3), revealing the presence of close $\text{H}\cdots\text{H}$ contacts, accounting for 30.7% of all intermolecular contacts. The FP plot in Fig. 6c has symmetrical peaks at the top left and bottom right with $d_e + d_i = 2.6$ Å (labeled 4 and 5), characteristic of $\text{C}-\text{H}\cdots\pi$ interactions (24.0%).

In the HS plotted over curvedness shown in Fig. 6d, the presence of flat regions indicates the existence of π -stacking interactions. Fig. 6e and 6f illustrate the $\text{C}\cdots\text{Cl}/\text{Cl}\cdots\text{C}$ and $\text{N}\cdots\text{H}/\text{H}\cdots\text{N}$ contacts, respectively. The other contacts shown in the two-dimensional fingerprint plots are $\text{C}\cdots\text{C}$ (6.2%), $\text{C}\cdots\text{Cl}/\text{Cl}\cdots\text{C}$ (4.1%) and $\text{N}\cdots\text{H}/\text{H}\cdots\text{N}$ (1.7%). The minimal contributions of the $\text{Cl}\cdots\text{Cl}$ (0.7%) and $\text{N}\cdots\text{C}/\text{C}\cdots\text{N}$ (0.2%)

intermolecular contacts mean they have a negligible impact on the packing.

6. Synthesis and crystallization

To prepare the title compound, a solution of 1,10-phenanthroline (0.090 g, 0.5 mmol) in ethanol (25 ml) and phenyltin trichloride (0.151 g, 0.5 mmol) in ethanol (25 ml) was refluxed for 24 h. The white precipitate that formed was removed by filtration. Colorless crystals were obtained after leaving a dichloroethane solution to stand for 7 d at room temperature. Yield: 85%. IR (KBr, cm^{-1}): 3054 (Ar—H), 3055 ($=\text{C}-\text{H}$), 1628 ($\text{C}=\text{N}$), 1430–1627 ($\text{C}=\text{C}$), 851 ($=\text{C}-\text{H}$), 448 (Sn—C), 423 (Sn—N).

7. Refinement

Crystal data, data collection and structure refinement details are summarized in Table 3. The C-bound H atoms were placed geometrically and refined as riding atoms [$\text{C}-\text{H} = 0.93 \text{ \AA}$ and $U_{\text{iso}}(\text{H}) = 1.2U_{\text{eq}}(\text{C})$].

Acknowledgements

We would like to thank the Ministry of Higher Education and Scientific Research of Algeria (MESRS Ministère de l'Enseignement Supérieur et de la Recherche Scientifique) and DGRSDT (Direction Generale de la Recherche Scientifique et du Developpement Technologique, Algérie) for financial support. We would like to thank team OMC of the University of Rennes1, CNRS, Institut des Sciences Chimiques de Rennes (ISCR)—UMR 6226, F-35000 Rennes, France for all their help during BT's internship and for the data collection.

References

Table 3 Experimental details.	
Crystal data	
Chemical formula	[Sn(C ₆ H ₅)Cl ₃ (C ₁₂ H ₈ N ₂)]
M_r	482.34
Crystal system, space group	Monoclinic, $P2_1/n$
Temperature (K)	150
a, b, c (Å)	9.1085 (9), 13.1958 (13), 14.9869 (14)
β (°)	102.261 (3)
V (Å ³)	1760.2 (3)
Z	4
Radiation type	Mo $K\alpha$
μ (mm ⁻¹)	1.91
Crystal size (mm)	0.4 × 0.3 × 0.2
Data collection	
Diffractometer	Bruker D8 VENTURE
Absorption correction	Multi-scan (<i>SADABS</i> ; Krause <i>et al.</i> , 2015)
No. of measured, independent and observed [$I > 2\sigma(I)$] reflections	23358, 4356, 3974
R_{int}	0.033
(sin θ/λ) _{max} (Å ⁻¹)	0.667
Refinement	
$R[F^2 > 2\sigma(F^2)], wR(F^2), S$	0.025, 0.055, 1.14
No. of reflections	3974
No. of parameters	217
H-atom treatment	H-atom parameters constrained
$\Delta\rho_{\text{max}}, \Delta\rho_{\text{min}}$ (e Å ⁻³)	0.44, -0.77
Computer programs: <i>APEX4</i> and <i>SAINT</i> (Bruker, 2014), <i>SHELXT2018/2</i> (Sheldrick, 2015a), <i>SHELXL2018/3</i> (Sheldrick, 2015b) and <i>OLEX2</i> (Dolomanov <i>et al.</i> , 2009).	
Kircher, P., Huttner, G., Heinze, K., Schiemenz, B., Zsolnai, L., Büchner, M. & Driess, A. (1998). <i>Eur. J. Inorg. Chem.</i> 1998 , 703–720.	
Klössener, J., Wiesemann, M., Neumann, B., Stammel, H. G. & Hoge, B. (2018). <i>Eur. J. Inorg. Chem.</i> pp. 3960–3970.	
Krause, L., Herbst-Irmer, R., Sheldrick, G. M. & Stalke, D. (2015). <i>J. Appl. Cryst.</i> 48 , 3–10.	
Lange, I., Moers, O., Blaschette, A. & Jones, P. G. (1997). <i>Z. Anorg. Allg. Chem.</i> 623 , 1665–1671.	
Lo, K. M., Lee, S. M. & Tiekkink, E. R. T. (2020). <i>Z. Kristallogr. New Cryst. Struct.</i> 235 , 695–697.	
Ma, C., Han, Y. & Li, D. (2004). <i>Polyhedron</i> , 23 , 1207–1216.	
Mo, C. J., Li, Z. Q., Que, C. J., Zhang, G. L., Zhu, Q. Y. & Dai, J. (2017). <i>Dyes Pigments</i> , 141 , 66–73.	
Najafi, E., Amini, M. M., Khavasi, H. R. & Ng, S. W. (2014). <i>J. Organomet. Chem.</i> 749 , 370–378.	
Najafi, E., Amini, M. M. & Ng, S. W. (2012). <i>Acta Cryst. E68</i> , m1544.	
Rebolledo, A. P., de Lima, G. M., Gambi, L. N., Speziali, N. L., Maia, D. F., Pinheiro, C. B., Ardisson, J. D., Cortés, M. E. & Beraldo, H. (2003). <i>Appl. Organomet. Chem.</i> 17 , 945–951.	
Ross, A. (2006). <i>Ann. N. Y. Acad. Sci.</i> 125 , 107–123.	
Sammes, P. G. & Yahioglu, G. (1994). <i>Chem. Soc. Rev.</i> 23 , 327–334.	
Sheldrick, G. M. (2015a). <i>Acta Cryst. A71</i> , 3–8.	
Sheldrick, G. M. (2015b). <i>Acta Cryst. C71</i> , 3–8.	
Spackman, M. A. & Jayatilaka, D. (2009). <i>CrystEngComm</i> , 11 , 19–32.	
Spackman, P. R., Turner, M. J., McKinnon, J. J., Wolff, S. K., Grimwood, D. J., Jayatilaka, D. & Spackman, M. A. (2021). <i>J. Appl. Cryst.</i> 54 , 1006–1011.	
Su, Z.-H., Zhou, B.-B., Zhao, Z.-F. & Ng, S. W. (2007). <i>Acta Cryst. E63</i> , m394–m395.	
Syed Annuar, S. N., Kamaludin, N. F., Awang, N. & Chan, K. M. (2021). <i>Front. Chem.</i> 9 , 657599.	
Tan, C. L., Lo, K. M. & Ng, S. W. (2009). <i>Acta Cryst. E65</i> , m717.	

supporting information

Acta Cryst. (2024). E80, 1039-1043 [https://doi.org/10.1107/S2056989024009150]

Crystal structure and Hirshfeld surface analysis of trichlorido(1,10-phenanthroline- κ^2N,N')phenyltin(IV)

Tarek Benlatreche, Mohamed Abdellatif Bensegueni, Georges Dénès, Stéphane Golhen and Hocine Merazig

Computing details

Trichlorido(1,10-phenanthroline- κ^2N,N')phenyltin(IV)

Crystal data

[Sn(C₆H₅)Cl₃(C₁₂H₈N₂)]

$M_r = 482.34$

Monoclinic, $P2_1/n$

$a = 9.1085$ (9) Å

$b = 13.1958$ (13) Å

$c = 14.9869$ (14) Å

$\beta = 102.261$ (3)°

$V = 1760.2$ (3) Å³

$Z = 4$

$F(000) = 944$

$D_x = 1.820$ Mg m⁻³

Mo $K\alpha$ radiation, $\lambda = 0.71073$ Å

Cell parameters from 9933 reflections

$\theta = 2.6\text{--}27.5^\circ$

$\mu = 1.91$ mm⁻¹

$T = 150$ K

Prism, clear yellowish colourless

0.4 × 0.3 × 0.2 mm

Data collection

Bruker D8 VENTURE
diffractometer

rotation images scans

Absorption correction: multi-scan
(SADABS; Krause et al., 2015)

23358 measured reflections

4356 independent reflections

3974 reflections with $I > 2\sigma(I)$

$R_{\text{int}} = 0.033$

$\theta_{\text{max}} = 28.3^\circ$, $\theta_{\text{min}} = 2.4^\circ$

$h = -12 \rightarrow 12$

$k = -17 \rightarrow 17$

$l = -19 \rightarrow 18$

Refinement

Refinement on F^2

Least-squares matrix: full

$R[F^2 > 2\sigma(F^2)] = 0.025$

$wR(F^2) = 0.055$

$S = 1.14$

3974 reflections

217 parameters

0 restraints

Primary atom site location: dual

Hydrogen site location: inferred from
neighbouring sites

H-atom parameters constrained

$w = 1/[\sigma^2(F_o^2) + (0.0068P)^2 + 2.7739P]$
where $P = (F_o^2 + 2F_c^2)/3$

$(\Delta/\sigma)_{\text{max}} = 0.001$

$\Delta\rho_{\text{max}} = 0.44$ e Å⁻³

$\Delta\rho_{\text{min}} = -0.77$ e Å⁻³

Special details

Geometry. All esds (except the esd in the dihedral angle between two l.s. planes) are estimated using the full covariance matrix. The cell esds are taken into account individually in the estimation of esds in distances, angles and torsion angles; correlations between esds in cell parameters are only used when they are defined by crystal symmetry. An approximate (isotropic) treatment of cell esds is used for estimating esds involving l.s. planes.

Refinement. Data collection was done using MoK α radiation with a D8 VENTURE Bruker-AXS diffractometer. Cell refinement and data reduction were performed using the SAINT program. The structure was solved using Olex2 (Dolomanov *et al.*, 2009) and the SHELXT (Sheldrick, 2018) program with intrinsic phasing. It was refined with the SHELXL (Sheldrick, 2015) package using least squares minimization.

Fractional atomic coordinates and isotropic or equivalent isotropic displacement parameters (\AA^2)

	<i>x</i>	<i>y</i>	<i>z</i>	$U_{\text{iso}}^*/U_{\text{eq}}$
Sn1	0.43722 (2)	0.69190 (2)	0.74892 (2)	0.01266 (5)
Cl3	0.65056 (6)	0.64521 (5)	0.87156 (4)	0.02106 (12)
Cl1	0.27434 (6)	0.73650 (4)	0.60281 (4)	0.01988 (11)
Cl2	0.42982 (7)	0.86043 (4)	0.80920 (4)	0.02232 (12)
N2	0.6229 (2)	0.73932 (15)	0.67755 (13)	0.0159 (4)
N1	0.5013 (2)	0.55247 (14)	0.67579 (13)	0.0152 (4)
C1	0.2682 (2)	0.61864 (17)	0.80618 (15)	0.0150 (4)
C17	0.6782 (2)	0.66479 (18)	0.63117 (15)	0.0161 (4)
C18	0.6156 (2)	0.56548 (18)	0.63148 (15)	0.0159 (4)
C7	0.4377 (3)	0.46156 (18)	0.67603 (16)	0.0201 (5)
H7	0.356976	0.453027	0.706415	0.024*
C2	0.1193 (3)	0.64428 (19)	0.77293 (17)	0.0212 (5)
H2	0.093114	0.687743	0.721470	0.025*
C3	0.0071 (3)	0.6065 (2)	0.81476 (18)	0.0263 (5)
H3	-0.094731	0.625359	0.792408	0.032*
C10	0.6716 (3)	0.48507 (19)	0.58645 (16)	0.0195 (5)
C8	0.4872 (3)	0.37828 (19)	0.63242 (17)	0.0247 (5)
H8	0.439814	0.314245	0.633125	0.030*
C16	0.6795 (3)	0.83217 (19)	0.67801 (17)	0.0218 (5)
H16	0.641490	0.884058	0.710796	0.026*
C13	0.7940 (2)	0.6826 (2)	0.58379 (16)	0.0199 (5)
C6	0.3047 (3)	0.55157 (19)	0.87977 (16)	0.0209 (5)
H6	0.406433	0.532876	0.902577	0.025*
C15	0.7934 (3)	0.8560 (2)	0.63175 (18)	0.0265 (5)
H15	0.831083	0.923282	0.633077	0.032*
C5	0.1922 (3)	0.5121 (2)	0.91977 (17)	0.0246 (5)
H5	0.216871	0.464759	0.968438	0.030*
C11	0.7900 (3)	0.5055 (2)	0.53918 (17)	0.0253 (5)
H11	0.828444	0.451887	0.508489	0.030*
C4	0.0444 (3)	0.5419 (2)	0.88845 (17)	0.0256 (5)
H4	-0.031568	0.517732	0.917810	0.031*
C9	0.6043 (3)	0.38929 (19)	0.58869 (17)	0.0249 (5)
H9	0.639571	0.332705	0.560140	0.030*
C12	0.8478 (3)	0.5997 (2)	0.53763 (17)	0.0259 (6)
H12	0.925432	0.611268	0.505372	0.031*

C14	0.8503 (3)	0.7819 (2)	0.58447 (18)	0.0261 (5)
H14	0.927037	0.797456	0.552514	0.031*

Atomic displacement parameters (\AA^2)

	U^{11}	U^{22}	U^{33}	U^{12}	U^{13}	U^{23}
Sn1	0.01200 (7)	0.01385 (8)	0.01264 (8)	0.00132 (5)	0.00377 (5)	-0.00003 (5)
Cl3	0.0157 (2)	0.0260 (3)	0.0195 (3)	0.0018 (2)	-0.0009 (2)	0.0031 (2)
Cl1	0.0206 (3)	0.0237 (3)	0.0144 (2)	0.0032 (2)	0.0017 (2)	0.0026 (2)
Cl2	0.0275 (3)	0.0174 (3)	0.0234 (3)	0.0021 (2)	0.0084 (2)	-0.0055 (2)
N2	0.0141 (9)	0.0171 (9)	0.0163 (9)	0.0006 (7)	0.0030 (7)	0.0007 (7)
N1	0.0159 (9)	0.0154 (9)	0.0149 (9)	0.0003 (7)	0.0045 (7)	-0.0011 (7)
C1	0.0152 (10)	0.0154 (10)	0.0150 (10)	-0.0009 (8)	0.0047 (8)	-0.0013 (8)
C17	0.0140 (10)	0.0211 (11)	0.0129 (10)	0.0018 (8)	0.0023 (8)	0.0012 (8)
C18	0.0151 (10)	0.0201 (11)	0.0125 (10)	0.0042 (8)	0.0029 (8)	0.0004 (8)
C7	0.0210 (11)	0.0177 (11)	0.0215 (12)	-0.0017 (9)	0.0041 (9)	0.0006 (9)
C2	0.0163 (11)	0.0258 (13)	0.0219 (12)	0.0025 (9)	0.0048 (9)	0.0037 (10)
C3	0.0150 (11)	0.0359 (15)	0.0301 (14)	-0.0020 (10)	0.0092 (10)	0.0010 (11)
C10	0.0199 (11)	0.0225 (12)	0.0149 (11)	0.0089 (9)	0.0012 (9)	-0.0015 (9)
C8	0.0323 (14)	0.0166 (11)	0.0238 (12)	0.0008 (10)	0.0027 (10)	-0.0016 (9)
C16	0.0204 (11)	0.0194 (12)	0.0245 (12)	-0.0003 (9)	0.0026 (9)	0.0030 (9)
C13	0.0123 (10)	0.0324 (13)	0.0153 (11)	0.0037 (9)	0.0035 (8)	0.0064 (9)
C6	0.0218 (11)	0.0234 (12)	0.0176 (11)	0.0031 (9)	0.0044 (9)	0.0028 (9)
C15	0.0242 (12)	0.0261 (13)	0.0287 (14)	-0.0061 (10)	0.0046 (10)	0.0091 (11)
C5	0.0320 (13)	0.0254 (13)	0.0171 (11)	-0.0062 (10)	0.0069 (10)	0.0053 (10)
C11	0.0217 (12)	0.0361 (15)	0.0192 (12)	0.0135 (11)	0.0071 (9)	-0.0016 (10)
C4	0.0262 (13)	0.0345 (14)	0.0195 (12)	-0.0106 (11)	0.0120 (10)	-0.0030 (10)
C9	0.0312 (13)	0.0212 (12)	0.0203 (12)	0.0118 (10)	0.0008 (10)	-0.0035 (9)
C12	0.0171 (11)	0.0440 (16)	0.0187 (12)	0.0082 (11)	0.0086 (9)	0.0027 (11)
C14	0.0165 (11)	0.0380 (15)	0.0244 (13)	-0.0031 (10)	0.0058 (9)	0.0114 (11)

Geometric parameters (\AA , $^\circ$)

Sn1—Cl3	2.4530 (6)	C10—C11	1.436 (3)
Sn1—Cl1	2.4419 (6)	C10—C9	1.409 (4)
Sn1—Cl2	2.4067 (6)	C8—H8	0.9500
Sn1—N2	2.2728 (19)	C8—C9	1.373 (4)
Sn1—N1	2.2802 (19)	C16—H16	0.9500
Sn1—C1	2.145 (2)	C16—C15	1.400 (3)
N2—C17	1.361 (3)	C13—C12	1.434 (4)
N2—C16	1.329 (3)	C13—C14	1.406 (4)
N1—C18	1.359 (3)	C6—H6	0.9500
N1—C7	1.333 (3)	C6—C5	1.393 (3)
C1—C2	1.384 (3)	C15—H15	0.9500
C1—C6	1.398 (3)	C15—C14	1.373 (4)
C17—C18	1.429 (3)	C5—H5	0.9500
C17—C13	1.411 (3)	C5—C4	1.386 (4)
C18—C10	1.410 (3)	C11—H11	0.9500

C7—H7	0.9500	C11—C12	1.352 (4)
C7—C8	1.401 (3)	C4—H4	0.9500
C2—H2	0.9500	C9—H9	0.9500
C2—C3	1.399 (3)	C12—H12	0.9500
C3—H3	0.9500	C14—H14	0.9500
C3—C4	1.379 (4)		
Cl1—Sn1—Cl3	165.07 (2)	C4—C3—H3	120.0
Cl2—Sn1—Cl3	91.82 (2)	C18—C10—C11	118.8 (2)
Cl2—Sn1—Cl1	93.08 (2)	C9—C10—C18	117.4 (2)
N2—Sn1—Cl3	82.62 (5)	C9—C10—C11	123.8 (2)
N2—Sn1—Cl1	83.27 (5)	C7—C8—H8	120.0
N2—Sn1—Cl2	90.30 (5)	C9—C8—C7	120.0 (2)
N2—Sn1—N1	72.77 (7)	C9—C8—H8	120.0
N1—Sn1—Cl3	85.10 (5)	N2—C16—H16	118.9
N1—Sn1—Cl1	86.12 (5)	N2—C16—C15	122.2 (2)
N1—Sn1—Cl2	163.04 (5)	C15—C16—H16	118.9
C1—Sn1—Cl3	96.23 (6)	C17—C13—C12	119.0 (2)
C1—Sn1—Cl1	96.68 (6)	C14—C13—C17	117.5 (2)
C1—Sn1—Cl2	100.76 (6)	C14—C13—C12	123.5 (2)
C1—Sn1—N2	168.92 (8)	C1—C6—H6	119.9
C1—Sn1—N1	96.16 (8)	C5—C6—C1	120.2 (2)
C17—N2—Sn1	115.73 (15)	C5—C6—H6	119.9
C16—N2—Sn1	125.32 (16)	C16—C15—H15	120.1
C16—N2—C17	118.9 (2)	C14—C15—C16	119.7 (2)
C18—N1—Sn1	115.71 (15)	C14—C15—H15	120.1
C7—N1—Sn1	124.69 (15)	C6—C5—H5	120.1
C7—N1—C18	119.6 (2)	C4—C5—C6	119.9 (2)
C2—C1—Sn1	118.52 (17)	C4—C5—H5	120.1
C2—C1—C6	119.3 (2)	C10—C11—H11	119.4
C6—C1—Sn1	122.04 (17)	C12—C11—C10	121.1 (2)
N2—C17—C18	118.0 (2)	C12—C11—H11	119.4
N2—C17—C13	122.3 (2)	C3—C4—C5	120.2 (2)
C13—C17—C18	119.7 (2)	C3—C4—H4	119.9
N1—C18—C17	117.7 (2)	C5—C4—H4	119.9
N1—C18—C10	122.1 (2)	C10—C9—H9	120.2
C10—C18—C17	120.2 (2)	C8—C9—C10	119.5 (2)
N1—C7—H7	119.3	C8—C9—H9	120.2
N1—C7—C8	121.4 (2)	C13—C12—H12	119.4
C8—C7—H7	119.3	C11—C12—C13	121.2 (2)
C1—C2—H2	119.8	C11—C12—H12	119.4
C1—C2—C3	120.3 (2)	C13—C14—H14	120.3
C3—C2—H2	119.8	C15—C14—C13	119.4 (2)
C2—C3—H3	120.0	C15—C14—H14	120.3
C4—C3—C2	120.0 (2)		
Sn1—N2—C17—C18	0.0 (3)	C18—N1—C7—C8	0.8 (3)
Sn1—N2—C17—C13	-179.75 (16)	C18—C17—C13—C12	-0.7 (3)

Sn1—N2—C16—C15	-179.48 (18)	C18—C17—C13—C14	179.1 (2)
Sn1—N1—C18—C17	-3.1 (3)	C18—C10—C11—C12	0.1 (4)
Sn1—N1—C18—C10	177.34 (17)	C18—C10—C9—C8	1.1 (3)
Sn1—N1—C7—C8	-177.42 (18)	C7—N1—C18—C17	178.6 (2)
Sn1—C1—C2—C3	-173.21 (19)	C7—N1—C18—C10	-1.0 (3)
Sn1—C1—C6—C5	174.69 (18)	C7—C8—C9—C10	-1.3 (4)
N2—C17—C18—N1	2.1 (3)	C2—C1—C6—C5	-0.8 (4)
N2—C17—C18—C10	-178.3 (2)	C2—C3—C4—C5	-1.7 (4)
N2—C17—C13—C12	179.1 (2)	C10—C11—C12—C13	0.6 (4)
N2—C17—C13—C14	-1.1 (3)	C16—N2—C17—C18	-179.9 (2)
N2—C16—C15—C14	-0.4 (4)	C16—N2—C17—C13	0.3 (3)
N1—C18—C10—C11	178.4 (2)	C16—C15—C14—C13	-0.5 (4)
N1—C18—C10—C9	0.1 (3)	C13—C17—C18—N1	-178.2 (2)
N1—C7—C8—C9	0.4 (4)	C13—C17—C18—C10	1.4 (3)
C1—C2—C3—C4	-1.2 (4)	C6—C1—C2—C3	2.4 (4)
C1—C6—C5—C4	-2.1 (4)	C6—C5—C4—C3	3.3 (4)
C17—N2—C16—C15	0.5 (3)	C11—C10—C9—C8	-177.2 (2)
C17—C18—C10—C11	-1.2 (3)	C9—C10—C11—C12	178.4 (2)
C17—C18—C10—C9	-179.5 (2)	C12—C13—C14—C15	-179.0 (2)
C17—C13—C12—C11	-0.3 (4)	C14—C13—C12—C11	179.9 (2)
C17—C13—C14—C15	1.2 (4)		

Hydrogen-bond geometry (Å, °)

D—H···A	D—H	H···A	D···A	D—H···A
C15—H15···Cl3 ⁱ	0.95	2.94	3.851 (1)	139
C5—H5···Cl3 ⁱⁱ	0.95	2.84	3.773 (2)	166
C9—H9···Cl1 ⁱⁱⁱ	0.95	2.87	3.683 (2)	144
C2—H2···Cl1	0.95	2.75	3.392 (2)	126
C6—H6···Cl3	0.95	2.86	3.411 (1)	124
C16—H16···Cl2	0.95	2.97	3.328 (3)	126
C7—H7···Cl2 ^{iv}	0.95	2.85	3.654 (1)	143
C12—H12···Cl2 ^v	0.95	2.97	3.693 (4)	133

Symmetry codes: (i) $-x+3/2, y+1/2, -z+3/2$; (ii) $-x+1, -y+1, -z+2$; (iii) $-x+1, -y+1, -z+1$; (iv) $-x+1/2, y-1/2, -z+3/2$; (v) $x+1/2, -y+3/2, z-1/2$.